

## **CHAPTER 2**

# **Thin Film Deposition and Characterization Techniques**

## **2. Thin Film Deposition and Characterization Techniques**

*Fabrication of copper indium diselenide thin film (CIS) solar cells requires excellent structural, optical and electrical properties of various semiconductor layers. This chapter discusses the thin film deposition methods used in this study for the growth of different semiconductor materials. The techniques used to investigate the structural features of the thin films viz. X-ray diffraction (XRD), Scanning electron microscopy (SEM), Transmission electron microscopy (TEM), and Atomic force microscopy (AFM) are also discussed. The optical characterization technique utilized to study the transmission of the grown semiconductor thin films is also discussed. Electrical measurements of semiconductor thin films are carried out using hot probe method, four point probe method, and Hall effect.*

### **2.1 Thin Film Deposition Techniques**

In this, section we focus on evaporation and sputtering, two of the most important methods used for depositing thin films. The objective of these deposition processes is, controllably transfer atoms from a source to a substrate where film formation and growth proceed atomistically. Experimental techniques used to deposit various thin film semiconducting layer in CIS thin film solar cell and their characterization techniques are discussed here.

#### **2.1.1 Thermal Evaporation Method**

A typical thermal evaporation system is schematically shown in figure 2.1. The system consists of an evaporation source that vaporizes the desired material and a substrate is located at an appropriate distance facing the evaporation source. Both the source and the substrate are located in a vacuum chamber. The substrate can be heated or electrically biased or rotated during deposition. The desired vapor pressure of source material can be generated by simply heating the source to elevated temperatures, and the concentration of the growth species in the gas phase can be easily controlled by varying the source temperature. The substrate temperature during the thin film deposition is measured using chromel-alumel thermocouple kept in good thermal contact with the substrate. The rate of deposition and thicknesses of the films are continuously monitored during the film deposition using a quartz crystal thickness

monitor DTM -101 (Hind Hi Vac., India). In order to improve crystallinity the evaporated thin films are deposited at different substrate temperatures ( $T_s$ ).

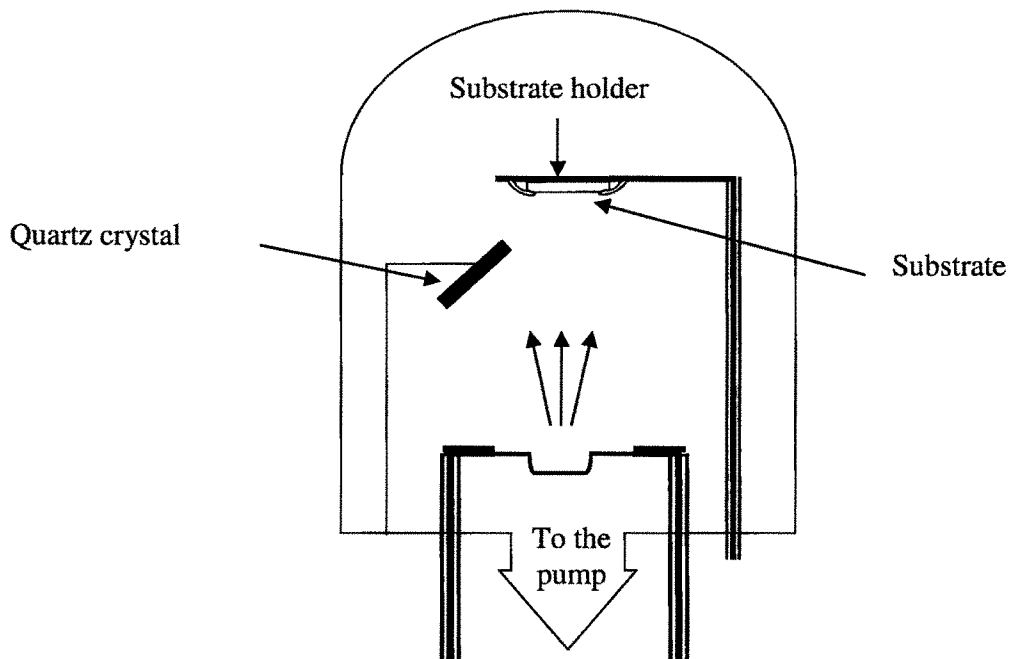


**Figure 2.1: A schematic of the thermal evaporation system.**

### **2.1.2 Flash Evaporation Method**

Flash evaporation technique is widely used by researchers to deposit binary/ternary semiconductor compound material owing to its simplicity and ease of operation. The schematic of flash system installed in vacuum coating unit is shown in figure 2.2. The system consists of a evaporation source and an electromagnetically vibrating feeder known as flash system, which supplies the powder material to the boat. Fine grains of pulverized material are fed into the preheated evaporation source kept at temperature higher than evaporation temperature of material via vibratory feeder. This result in uniform film deposition on substrates kept at different  $T_s$ .

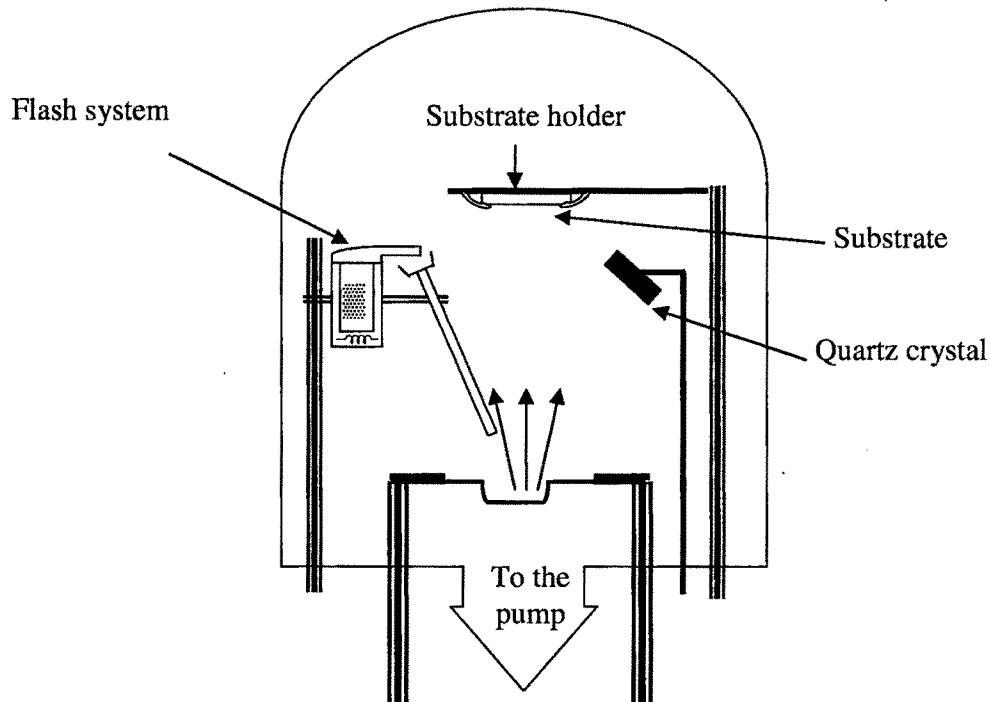


**Figure 2.2: The flash evaporation system installed in the vacuum coating unit.**

### **2.1.3 Sputtering Technique**

Sputtering is one of the most versatile deposition techniques used for the deposition of transparent conducting oxides (TCO). When sputtering is compared to other techniques, sputtering produces films with higher purity and better-controlled composition. It also produces films with greater adhesive strength, homogeneity and permits better control of film thickness. Sputtering processes involves the creation of gas plasmas (usually an inert gas such as argon) between an anode and cathode. The cathode is used as the source of sputtered particles whereas the anode is usually the substrate holder. The source material is subjected to intense bombardment by ions. Using the momentum transferred from the bombarding ions, particles are ejected from the surface of the source (cathode) and then diffuse away from it, depositing a thin film onto the substrate. Sputtering is usually performed at pressures of  $10^{-2}$ - $10^{-3}$  Torr.

In standard sputtering processes there are usually two modes of powering the sputtering system. These two modes are direct current (DC) or by radio frequency (RF). In DC sputtering, a direct voltage is applied between the cathode and the anode. This method works well with conductive targets (molybdenum, silver, aluminum, etc). The second method involves the use of a radio frequency source with a typical frequency of 13.56 MHz. This

method is referred for both conductive as well as non-conductive targets. However, with the ever increasing demand for increased sputter rates it is found that the application of magnets above the target increased the sputtering rate and decreased the unintentional substrate heating. Generally this method is known as RF magnetron sputtering. The schematic diagram of RF magnetron sputtering is shown in figure 2.3. The system consists of, a RF generator, a matching unit, the vacuum coating unit, and the gas inlet system. Each part plays a specific role in the sputter process as outlined below.

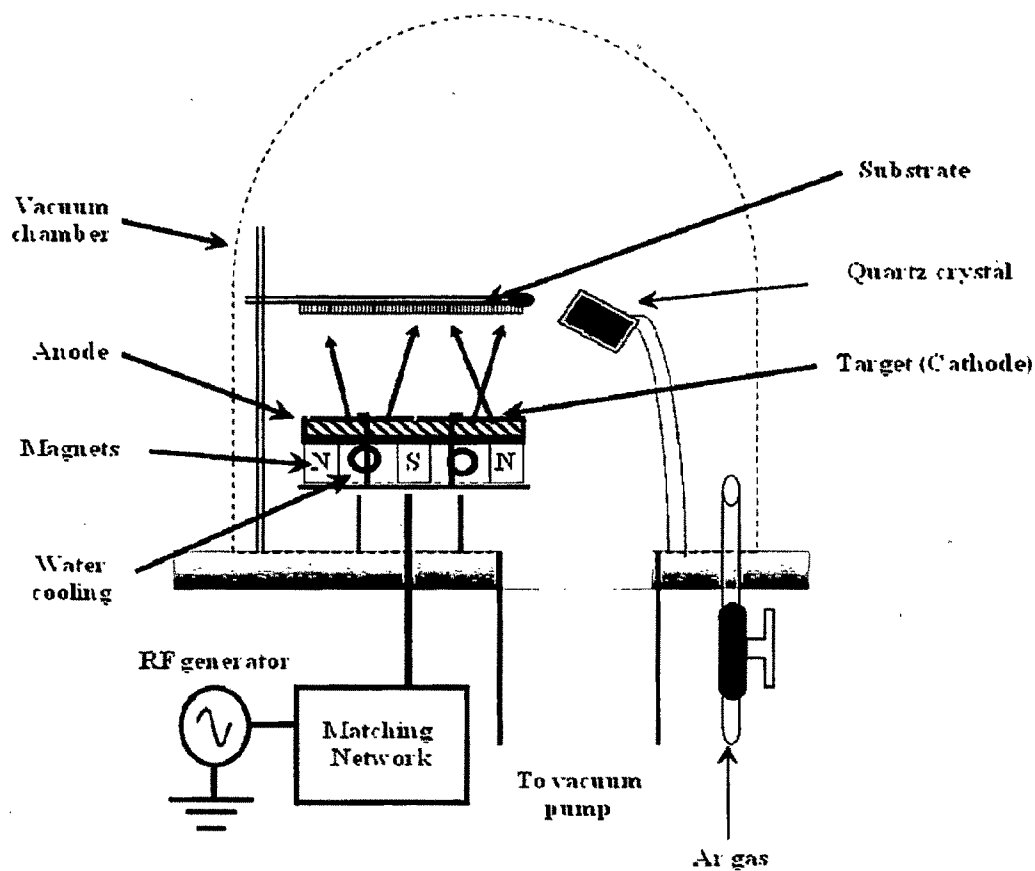


**Figure 2.3: A Schematic showing the principle of RF sputtering system.**

- RF generator: A Huttlinger (Germany) PFG 600 RF generator with a maximum output of 600 W is used to deposit the Mo and ZnO thin films. The RF generator creates a dense glow discharge (plasma) due to bias potential built up on the target surface. The negative bias potential of the target results in the ion bombardment, i.e., sputtering of the target.
- Matching unit: A matching unit is connected with the magnetron unit, which is kept inside the vacuum chamber. To achieve an efficient energy transfer from the RF

generator at a nominal load of approximately 50  $\Omega$ , the matching unit is kept closer to the chamber.

- Vacuum coating unit: A high vacuum coating unit (Model: 15F6 from Hind High Vacuum Co. (P) Ltd.) equipped with water cooled target holder (cathode electrode), adjustable substrate holder and accessory. There are two pumps, a rotary pump and a diffusion pump to achieve a base pressure of  $10^{-5}$  Torr.
- Gas inlet system: Combination of rotameter and needle valve is used to control the flow of the argon gas used for the sputtering process.

## 2.2 Thin Film Characterization Techniques

A wide variety of characterization techniques are used to evaluate the material quality of the semiconductor thin films. The structural properties of the polycrystalline films are studied by scanning electron microscopy (SEM) and atomic force microscopy (AFM) in non-contact mode while the presence of crystalline phases by X-ray diffraction (XRD) and transmission electron microscopy (TEM). Composition measurements are made by energy dispersive analysis of X-rays (EDAX) equipped with SEM. The electrical properties of the materials are investigated by Four-point probe and Hall Effect measurements. The optical properties of the films are studied using transmission measurements.

### 2.2.1 X-Ray Diffraction (XRD)

X-ray diffraction (XRD) is a very powerful experimental technique for studying crystal structures of solids and thin films. The preferred orientation of crystallites grown in semiconducting thin-film samples used for CIS solar cell fabrication viz. CIS, CdS and ZnO is obtained from XRD analysis.

In XRD analysis, a collimated beam of X-rays, with a wavelength typically ranging from 0.7 to 2 Å, is incident on a specimen and is diffracted by the crystalline phases in the specimen according to Bragg's law:

$$2d\sin\theta = n\lambda \quad (2.1)$$

where  $d$  is the spacing between atomic planes in the crystalline phase and  $\lambda$  is the X-ray wavelength. The intensity of the diffracted X-rays is measured as a function of the diffraction angle  $\theta$ . This diffraction pattern is used to identify the crystalline phases present in thin films.

The crystallite size,  $d$ , can be estimated from the peak width in XRD pattern using the Scherrer's formula [77]:

$$d = \frac{K\lambda}{B\cos\theta} \quad (2.2)$$

where  $\lambda$  is the X-ray wavelength ( $\lambda = 0.15418$  nm with Cu  $K\alpha$  radiation)  $B$  is the full width at half maximum (FWHM) of a diffraction peak,  $\theta$  is the diffraction angle, and  $K$  is the Scherrer's constant of the order of unity for usual crystal and thin films. It is important to note that X-ray diffraction only provides the collective information of the particle sizes and usually requires a sizable amount of powder and thickness of thin films. Details of XRD method is outlined by Cullity and Stock [78]. The structural characterization of the semiconducting thin films in this work are carried out using Shimadzu Lab X 6000 X- ray diffractometer, with Cu  $K\alpha$  ( $\lambda = 0.15418$  nm) radiation, operated at 40 kV voltage and current of 20 mA, shown in figure 2.4.



**Figure 2.4:** Shimadzu Lab X 6000 X- ray diffractometer.

### **2.2.2 Scanning Electron Microscopy (SEM)**

The morphological and compositional characterization of the semiconducting thin films in this work are carried out using scanning electron microscope ESEM, 30XL, Philips make, equipped with energy dispersive analysis of x-rays (EDAX) facilities operated at 30 keV with standardless ZAF quantification.

A schematic representation of a typical SEM is shown in figure 2.5. Electrons emitted from an electron gun pass through a series of lenses to be focused and scanned across the sample. Electron beams having energies ranging from 0.5 keV to 30 keV, is focused by one or two condenser lenses. The beam then passes through pairs of scanning coils or pairs of deflector plates in the electron column, typically in the final lens.

When the electron beam interacts with the sample, the electrons lose energy by repeated random scattering and absorption. The energy exchange between the electron beam and the sample results in the reflection of high-energy electrons by elastic scattering, emission of secondary electrons by inelastic scattering and the emission of electromagnetic radiation, each of which can be detected by detectors. The beam current absorbed by the specimen can also be detected and used to create images of the distribution of specimen current. Electronic amplifiers of various types are used to amplify the signals, which are displayed as variations in brightness on a cathode ray tube (CRT). The raster scanning of the CRT display is synchronized with that of the beam on the specimen in the microscope, and the resulting image is therefore a distribution map of the intensity of the signal being emitted from the scanned area of the specimen. The image can be digitally captured and displayed on a computer monitor and saved to a computer's hard disk.

### **2.2.3 Energy Dispersive Analysis of X-rays (EDAX)**

The most common non destructive technique used for the compositional analysis of thin films is electron probe micro-analysis (EPMA), sometimes also called energy dispersive X-ray spectroscopy (EDAX or EDS) generally attached with SEM's. There are two common methods to record the spectra of the emitted characteristic radiation. The first is to measure the whole energy spectrum simultaneously with an energy sensitive detector. The second option is to use a goniometer and an analyzing crystal with  $\theta$ - $2\theta$  coupling and to assign a measured intensity to a  $2\theta$  position. By means of the Bragg equation  $2d \sin\theta = n\lambda$ , the energy of a measured peak can then be determined from the  $2\theta$ -position of the detector.

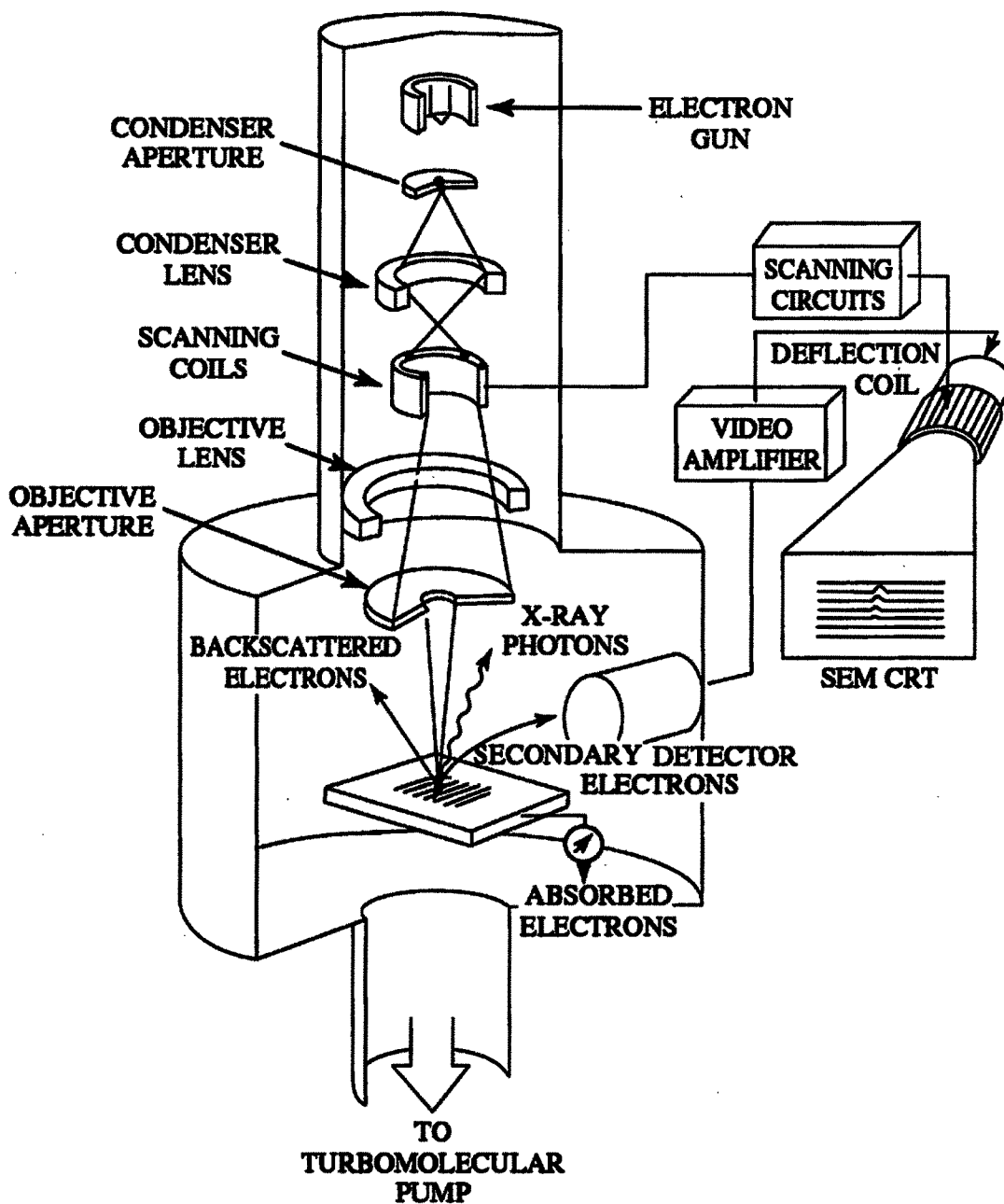


Figure 2.5: Schematic representation of scanning electron microscope.

The first technique, the energy dispersive spectrometry, is known as EDS or EDAX, while the second approach is called wavelength dispersive spectrometry (WDS or WDX). We have used EDAX for compositional analysis of CIS and CdS thin films.

#### 2.2.4 Transmission Electron Microscopy (TEM)

Transmission electron microscope (TEM) is, in principle, similar to optical microscopes; both contain a series of lenses to magnify the surface of the test sample. Transmission electron

microscopy is originally used for higher magnification. Later, analytical capabilities such as electron energy loss detectors and X-ray detectors are added to the instrument and the technique is now also known as stands for either “microscopy” or “microscope.”

A schematic of a transmission electron microscope is shown in figure 2.6. Electrons from an electron gun are accelerated to high voltages-focused on the sample by the condenser lenses. The sample is placed on a small copper grid, a few mm in diameter. The static beam has a diameter of a few microns. The sample must be sufficiently thin (a few tens to a few hundred nm) to be transparent to electrons. The transmitted and forward scattered electrons form a diffraction pattern in the back focal plane and a magnified image in the image plane. With additional lenses, either the image or the diffraction pattern is projected onto a fluorescent screen for viewing or electronic or photographic recording. The ability to form a diffraction pattern yields structural information.

Selected area (electron) diffraction (abbreviated as SAD or SAED), is a crystallographic experimental technique that can be performed inside a transmission electron microscope (TEM). SAD pattern of CIS and CdS thin films are obtained in this study using the JEOL make TEM, JEM-2100. To obtain SAD pattern the wavelength of high-energy electrons is incident on very thin, ~50-100 nm, semiconducting film. The atoms in the film act as a diffraction grating to the electrons, which are diffracted. That is, some fraction of them will be scattered to particular angles, determined by the crystal structure of the sample, while others continue to pass through the sample without deflection. As a result, the image on the screen of the TEM will be a series of spots known as the selected area diffraction pattern, (SAD) shown in figure 3.6 and 4.3. Here, each spot corresponds to a satisfied diffraction condition of the sample's crystal structure.

### **2.2.5 Atomic Force Microscopy (AFM)**

Atomic force microscope is a versatile tool to investigate the morphology and growth structure of the thin films. We have investigated the surface morphology of semiconducting thin films using atomic force microscope CP II research head, Veeco (USA) make, in non contact mode.

The operating principle of AFM is illustrated in figure 2.7. The instrument consists of a cantilever with a sharp tip mounted on its one end. The cantilever is usually formed from silicon, silicon oxide or silicon nitride and is typically 100  $\mu\text{m}$  long, 20  $\mu\text{m}$  wide, and 0.1  $\mu\text{m}$

thick. The vertical sensitivity of cantilever depends on its length, which can be sensed by one or several methods [79]. The cantilever motion causes the reflected light to impinge on different segments of the photodiode.

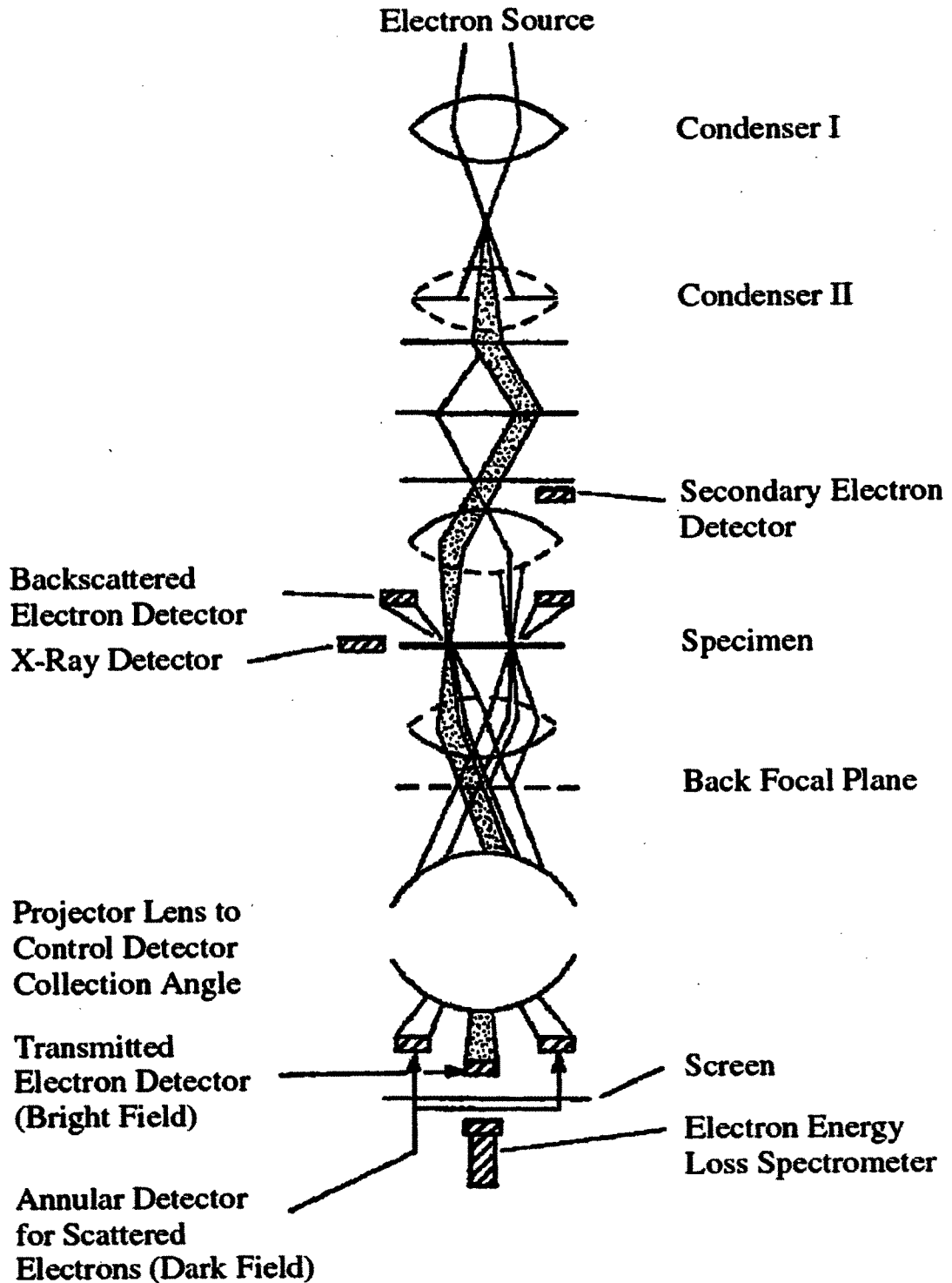
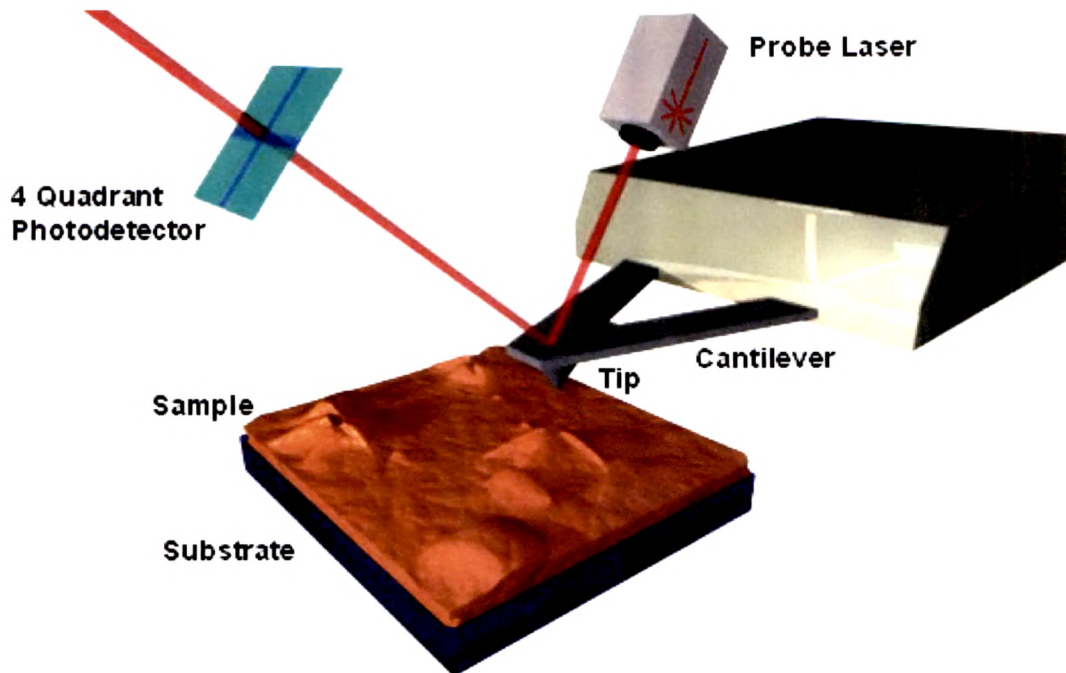
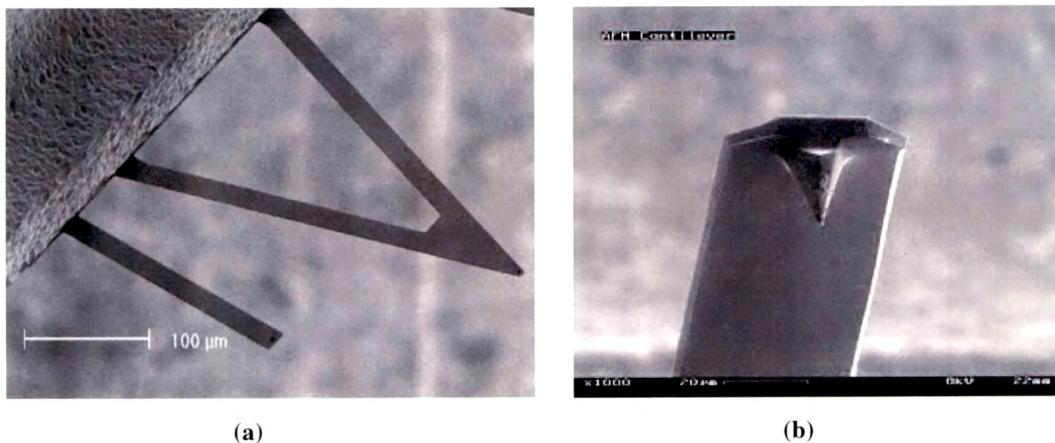


Figure 2.6: Schematic representation of transmission electron microscope.



**Figure 2.7: Schematic illustration of atomic force microscope.**

Cantilevers come in two common shapes as shown in figure 2.8. The three common modes of operation of AFMs are, 1) Contact mode, 2) Non- contact mode, and 3) Tapping mode.



**Figure 2.8: AFM cantilevers (a) V-Shaped type (b) Beam type.**

In the contact mode, the probe tip is dragged across the surface and the resulting image is a topographical map of the sample surface. The dragging motion of the probe tip, combined with adhesive forces between the tip and the surface can distort measurement data and damage the sample. In the non-contact mode, the instrument senses Van-der Waal attractive forces between the surface and the probe tip held above the sample surface. Unfortunately, these forces are substantially weaker than the contact mode forces, so weak in fact that the tip must be given a small oscillation and ac detection methods are used to detect

the small forces between tip and sample. Non-contact mode provides lower resolution than either contact or tapping mode. Tapping mode imaging overcomes the limitations of the conventional scanning modes by alternately placing the tip in contact with the surface to provide high resolution and then lifting the tip off the surface to avoid dragging the tip across the surface [80]. During scanning, the vertically oscillating tip alternately contacts the surface and lifts off, generally at a frequency of 50 to 500 kHz. Tapping mode imaging works well for soft, adhesive, or fragile samples, allowing high resolution topographic imaging of sample surfaces that are easily damaged or otherwise difficult to image by other AFM techniques.

### 2.2.6 Optical Transmission Measurements

The optical transmission of various semiconducting thin films, viz. CIS, CdS and AZO is used to determine the energy bandgap of the material. During transmission measurements light is incident on the sample and the transmitted light is measured as a function of wavelength. The transmitted light,  $I_t$ , can be measured absolutely or the ratio of transmitted to incident light,  $I_0$ . The absorption coefficient is determined using Lambert's law [81],

$$\ln\left(\frac{I_0}{I_t}\right) = \alpha d \quad (2.3)$$

where,  $d$  is the film thickness,  $I_0$  and  $I_t$  are the intensity of the incident and the transmitted light, and  $\alpha$  is the absorption coefficient. The energy bandgap of semiconductor can be derived by calculating the absorption coefficient ( $\alpha$ ) as a function of the photon energy. For indirect bandgap semiconductors,  $\alpha^{1/2}$  is plotted against  $h\nu$ , the extrapolated intercept on the  $h\nu$  axis yields the semiconductor bandgap. Such a plot is sometimes referred to as a Tauc plot. For direct bandgap semiconductors  $\alpha^2$  is plotted against  $h\nu$  and the bandgap is again determined from the extrapolated intercept. The schematic diagram of transmission measurement set-up used in this thesis is shown in the figure 2.9.

Here, a Tungsten-Halogen lamp is used as a polychromatic light source. The light from the lamp is focused on the monochromator input slit using a convex lens. We have used 1/8m monochromator (CM110). The output beam from the monochromator is chopped using a mechanical chopper. This chopped beam is then incident on the sample near-normal geometry and the transmitted beam is directed to the photo-detector. The detector measures the intensity of the transmitted beam with the help of lock-in amplifier (SR-530). The monochromator and the lock-in amplifier have been interfaced with the computer using COM port and GPIB, respectively. The experiment is automated using LabVIEW.

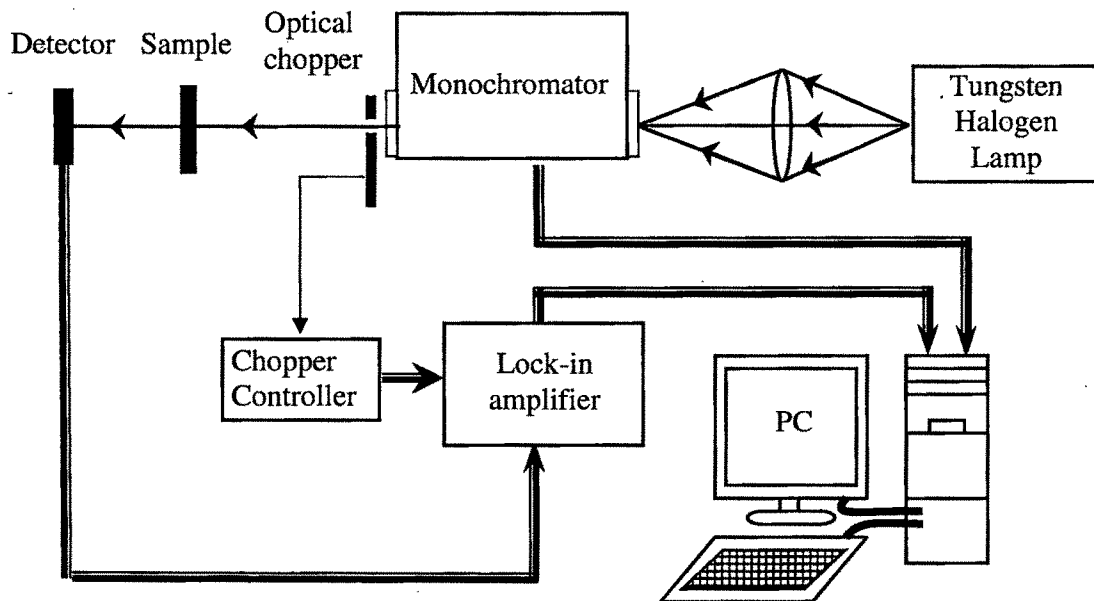


Figure 2.9: Set up for transmission measurements.

## 2.2.7 Electrical Measurements

### 2.2.7.1 Hot-Probe Method

The semiconductor conductivity can be determined using hot probe method. The schematic diagram for hot probe method is shown in figure 2.10.

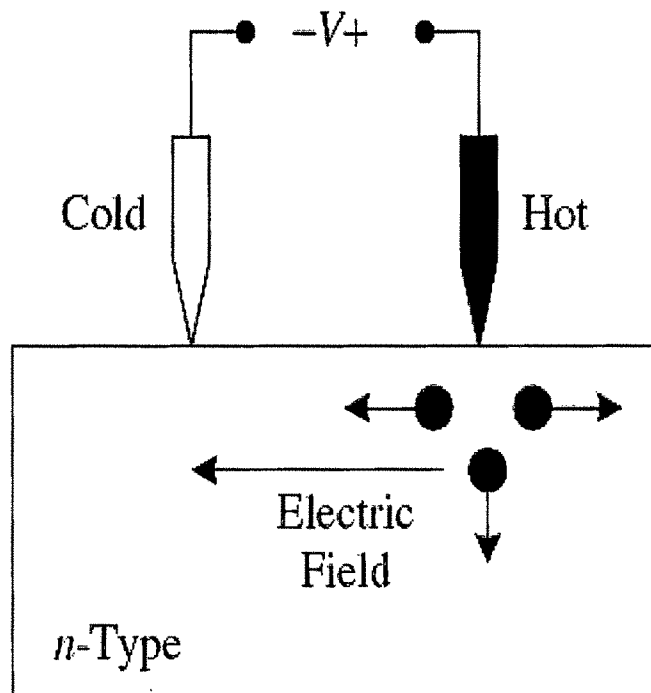


Figure 2.10: Schematic diagram of hot probe method.

In the hot or thermoelectric probe method the conductivity type is determined by the sign of the thermal emf or Seebeck voltage generated by a temperature gradient. Two probes contact the sample surface: one is hot the other is cold. Electrons diffuse from the hot to the cold region setting up an electric field that opposes the diffusion. The electric field produces a potential detected by the voltmeter with the hot probe positive with respect to the cold probe.

### 2.2.7.2 Four-point Probe Method

The four-point probe is commonly used technique to measure the semiconductor resistivity. It is an absolute measurement without recourse to calibrated standards and is sometimes used to provide standards for other resistivity measurements. The schematic diagram of four-point probe measurement technique is shown in figure 2.11. It is seen that by applying current  $I$  between terminal 1 and 4 (outer terminals in the figure) and measuring voltage  $V$  across terminal 2 and 3 (inner terminals) one can calculate sheet resistance ( $R_{sh}$ ) of the film using following equation.

$$R_{sh} = \frac{\pi}{\ln 2} \left( \frac{V}{I} \right) \quad (2.4)$$

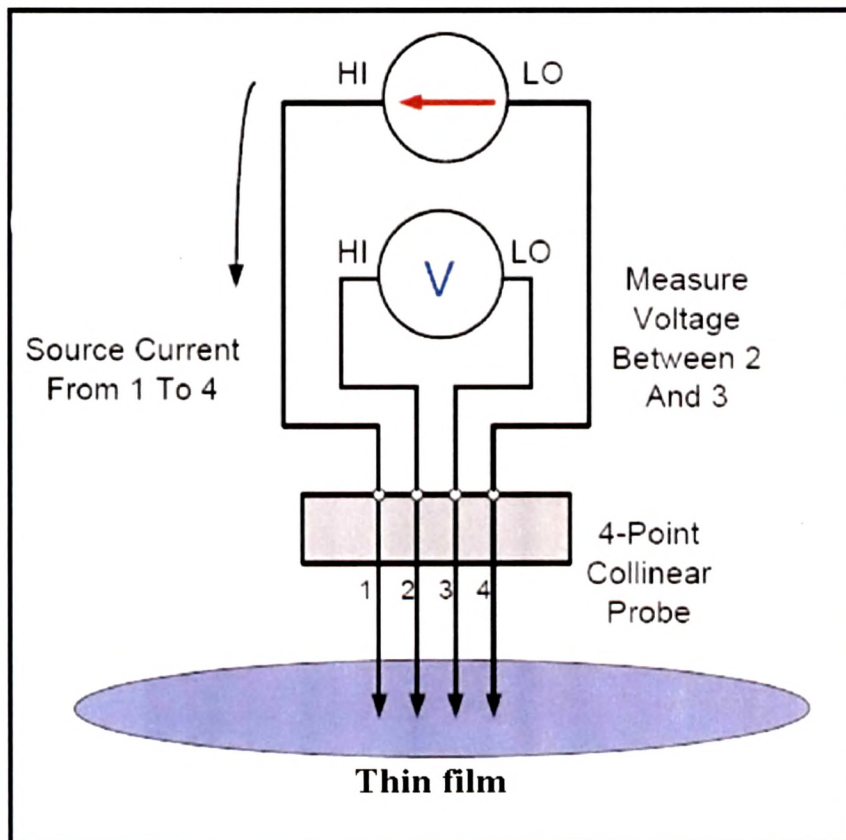


Figure 2.11: Schematic diagram of four point probe method.

### 2.2.7.3 Hall Effect Measurement

The Hall effect measurement technique has found wide application in the characterization of semiconductor materials because it gives the resistivity, the carrier density, and the carrier mobility. A detailed discussion of the Hall effect and its application to mobility measurements is given in [82] and explained the next paragraphs.

Consider the p-type semiconductor sample in figure 2.12. A current  $I$  flows in the X-direction, indicated by the holes flowing to the right and a magnetic field  $B$  is applied in the Z-direction. The current is given by,

$$I = qApv_x = qwdpv_x \quad (2.5)$$

The voltage along the x-direction, indicated by  $V_p$ , is

$$V_p = \rho \left( \frac{S}{wd} \right) I \quad (2.6)$$

from which the resistivity is derived as,

$$\rho = \frac{wd}{S} \frac{V_p}{I} \quad (2.7)$$

Consider now the motion of holes in a uniform magnetic field strength  $B$ . The force on the holes is given by the vector expression,

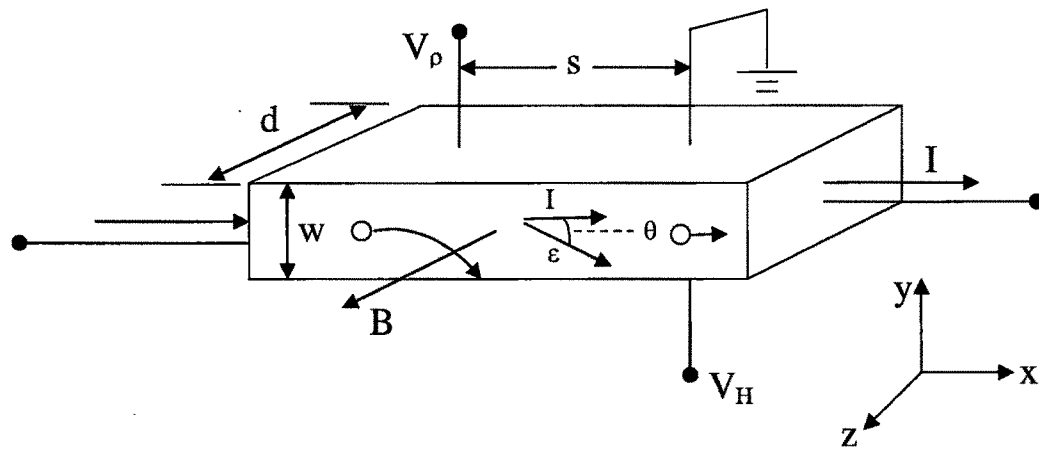


Figure 2.12: Schematic illustrating Hall effect in P type sample.

$$F = q[E + (v \times B)] \quad (2.8)$$

The magnetic field in conjunction with the current deflects some holes to the bottom of the sample, as indicated in figure 2.12. For n-type samples, the electrons are also deflected to the bottom of the sample for the same current direction as that in figure 2.12 because they

flow in the opposite direction to holes and have opposite charge. In the y-direction there is no net force on the holes since no current can flow in that direction and  $F_y = 0$ . Combining equations (2.8) and (2.5) gives,

$$E_y = Bv_x = \frac{BI}{qwdp} \quad (2.9)$$

The electric field in the y-direction produces the Hall voltage  $V_H$ ,

$$\int_0^{V_H} dV = V_H = \int_w^0 E_y dy = - \int_w^0 \frac{BI}{qwdp} = \frac{BI}{qdp} \quad (2.10)$$

The Hall coefficient  $R_H$  is defined as,

$$R_H = \frac{dV_H}{BI} \quad (2.11)$$

The Hall mobility  $\mu_H$  is defined by,

$$\mu_H = \frac{R_H}{\rho} = R_H \sigma \quad (2.12)$$

For extrinsic p-type and n-type semiconductors, respectively, Hall mobility can differ significantly from conductivity mobility.

## Conclusions

This chapter outlines the thin film deposition methods used to deposit various semiconducting thin films for thin film CIS solar cell device fabrication. The structural, morphological, characterization methods of thin films viz. XRD, TEM, SEM, AFM, are discussed in this chapter. The optical and electrical methods to characterize semiconducting thin films are also discussed.